



HAL
open science

Impedance of an induction coil accounting for the end-effect in eddy-current inspection of steam generator tubes

Konstantinos Pipis, Anastassios Skarlatos, Dominique Lesselier, Theodoros Theodoulidis

► To cite this version:

Konstantinos Pipis, Anastassios Skarlatos, Dominique Lesselier, Theodoros Theodoulidis. Impedance of an induction coil accounting for the end-effect in eddy-current inspection of steam generator tubes. N. Yusa, T. Uchimoto, and H. Kikuchi. Electromagnetic Nondestructive Evaluation (XIX), 41, IOS Press, pp.237-244, 2016, Studies in Applied Electromagnetics and Mechanics, 978-1-61499-638-5 (print) | 978-1-61499-639-2 (online). 10.3233/978-1-61499-639-2-237 . hal-01334098

HAL Id: hal-01334098

<https://centralesupelec.hal.science/hal-01334098>

Submitted on 30 Jan 2024

HAL is a multi-disciplinary open access archive for the deposit and dissemination of scientific research documents, whether they are published or not. The documents may come from teaching and research institutions in France or abroad, or from public or private research centers.

L'archive ouverte pluridisciplinaire **HAL**, est destinée au dépôt et à la diffusion de documents scientifiques de niveau recherche, publiés ou non, émanant des établissements d'enseignement et de recherche français ou étrangers, des laboratoires publics ou privés.

Impedance of an Induction Coil Accounting for the End-Effect in Eddy-Current Inspection of Steam Generator Tubes

Konstantinos PIPIS ^{a,1}, Anastassios SKARLATOS ^a, Theodoros THEODOULIDIS ^b
and Dominique LESSELIER ^c

^a *CEA, LIST, Centre de Saclay, Gif-sur-Yvette cedex, F-91191, France*

^b *Department of Mechanical Engineering, University of Western Macedonia, Kozani,
50100, Greece*

^c *Laboratoire des Signaux et Systèmes, UMR8506 (CNRS-CentraleSupélec-U. Paris
Sud), 91192 Gif-sur-Yvette cedex, France*

Abstract. A fast model for the eddy-current signal calculation of thin cracks at the vicinity of a conducting tube edge is presented. The model is based on the surface integral equation formalism using a dedicated Green's function. The approach followed for the construction of the Green's kernel and the primary field is the Truncated Region Eigenfunction Expansion (TREE) method.

Keywords. tube eddy-current inspection, TREE method, Surface Integral Method

Introduction

Eddy-current testing of parts for industrial applications such as steam generator tubes has led to the need for fast and precise modelling methods. The integral equation formalism is an approach that can give fast results for a large number of probe positions since, comparing to the finite element method (FEM), there is no need to discretise the entire geometry but only the defects surface (Surface Integral Method - SIM) [1], in the case of a thin crack, or its volume (Volume Integral Method - VIM) [2] in the case of volumetric defects. This formulation requires the calculation of the electric field in the absence of the flaw (primary field) as well as the Green's function expression corresponding to the geometry of the unflawed piece. In [3] the primary field in a conductor with a borehole as a function of the position of a coil in it is calculated and [4] presents the steps for the Green's function construction for the case of a conducting right-angled corner by means of the Truncated Region Eigenfunction Expansion (TREE) method is presented. The TREE method consists a powerful tool for the solution of low-frequency electromagnetic

¹Corresponding Author: Konstantinos Pipis, CEA, LIST, Centre de Saclay, F-91191 Gif-sur-Yvette cedex, France; E-mail: konstantinos.pipis@cea.fr.

problems and it is followed in this work in order to develop a fast and accurate model for the inspection of tubular geometries.

1. Theoretical Analysis

1.1. Assumptions and Formalism

A conducting, non-magnetic and homogeneous semi-infinite tube of thickness $b_2 - b_1$, conductivity σ and permeability μ_0 is considered, as shown in Fig. 1. The tube contains a thin crack at the vicinity of its edge. We define as thin crack a flaw of a very small opening compared to the size of the probe and the skin depth, which acts as a barrier to electric current. Thus, a thin crack in a conducting material where eddy-currents are induced can be represented by a distribution of electric dipoles. The considered time dependence convention of the harmonic excitation is of the form $e^{j\omega t}$. The frequencies used in the eddy-current applications are low enough in order for the quasi-static approximation to be applicable.

The magnetic flux density \mathbf{B} in air is expressed by a scalar potential $\mathbf{B} = \nabla\phi$ which satisfies the Laplace equation $\nabla^2\phi = 0$. Furthermore, as far as the formalism in the conducting regions is concerned, the magnetic flux density is expressed by a second order vector potential approach, i.e. $\mathbf{B} = \nabla \times \nabla \times \mathbf{W}$, with $\mathbf{W} = W_a\mathbf{e}_z + \mathbf{e}_z \times \nabla W_b$. $W_{a,b}$ satisfy the Helmholtz equation $(\nabla^2 - k^2)W_{a,b} = 0$, where $k^2 = j\omega\mu_0\sigma$.

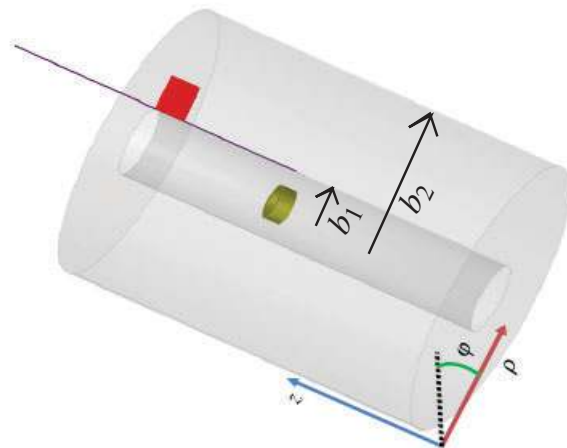


Figure 1. Inspection of a conducting tube of inner and outer radius b_1 and b_2 , respectively, with a crack at the edge of the tube. The flaw surface is on the $\rho - z$ plane with a narrow azimuthal opening.

1.2. Primary field and Green's function calculation

In this subsection the analysis for the primary field and the Green's function calculation is presented. The primary field is defined as the electric field induced in the test-piece in the absence of a flaw. Furthermore, an electric-electric dyad \mathbf{G} is a tensor of second rank corresponding to the electric field radiated by an infinitesimal electric dipole. This operator is the kernel of the integral formulation used to calculate the eddy-current testing (ECT) signal due to the flaw. Since we are concerned with a thin crack we consider

electric dipoles of only one direction and, thus, we need to calculate a Green's function instead of the whole tensor. Regarding the crack orientation, the electric dipoles are considered along the φ -direction and thus, only the $G^{\varphi\varphi}$ function needs to be calculated.

The two problems that we examine in this work differ only in the considered field source. In order to calculate the primary field for the configuration of Fig. 1 a coil of inner radius r_a , outer radius r_b , height H_c and N number of turns is considered. The coil is excited with an alternating current $e^{j\omega t}$. Additionally, in order to construct the Green's function, an electrical dipole along φ is assumed, with respect to the direction of the crack. In both cases, the geometry is separated in different regions as shown in Fig. 2, taking into account the expression of the potentials in each region.

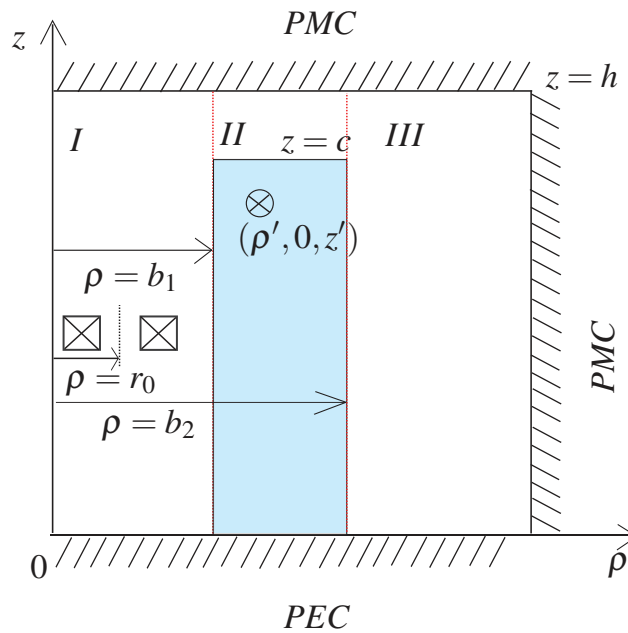


Figure 2. Separation of the configuration in different regions.

In order to facilitate the analysis the approach followed for the calculation of the electric field is divided in two steps. In this configuration we separate the field in two terms; the term that we call source field and the reflection term. In the case of the primary field calculation, the source field refers to the field radiated from the coil in the free space ignoring the presence of the tube, whereas the reflection terms represent the perturbation of the field due to the conducting tube. In the case of the Green's function construction the term "source field" is conventionally used in order to express the field induced by the electric dipole as well as the field reflected by the horizontal interface of the tube, whereas the "reflection terms" describe the perturbation by the radial interfaces of the test-piece. The notation $\tilde{\phi}, \tilde{W}_{a,b}$ is used for the potentials corresponding to the source terms and the potentials $\Delta\tilde{\phi}, \Delta\tilde{W}_{a,b}$ represent the reflection terms.

The cylindrical symmetry of the inspected geometry as well as the truncation of the solution domain according to the TREE method allow us to express the field as a series expansion. The modal decomposition in this analysis is done using sines and cosines or exponential functions along z , Bessel or modified Bessel functions along ρ and exponential functions along φ depending on the geometry of each of the two steps described before.

$$\phi = \sum_{m=-\infty}^{\infty} e^{jm\varphi} \sum_{n=1}^{\infty} (\tilde{\phi}_{mn} + \Delta\tilde{\phi}_{mn}) \quad (1)$$

$$W_{a,b} = \sum_{m=-\infty}^{\infty} e^{jm\varphi} \sum_{n=1}^{\infty} (\tilde{W}_{a,bmn} + \Delta\tilde{W}_{a,bmn}) \quad (2)$$

1.2.1. Green's function construction

We first present the analysis for the Green's function construction, which is more complex than the primary field calculation. According to the first step of the analysis, the source terms are calculated, as it is already mentioned. In this case, the field source is the electric dipole located in region *II*, whereas the coil is ignored. The expression of the potentials is as

$$\tilde{\phi}_{mn}^{II} = A_{mn} e^{-\kappa_n(z-z_0)} J_m(\kappa_n \rho); \quad z > c \quad (3)$$

$$\tilde{W}_{a_{mn}}^{II+} = [B_{mn} e^{-v_n(z-z_0)} + C_{mn} e^{v_n(z-z_0)}] J_m(\kappa_n \rho); \quad z' \leq z \leq c \quad (4)$$

$$\tilde{W}_{b_{mn}}^{II+} = [D_{mn} e^{-r_n(z-z_0)} + E_{mn} e^{r_n(z-z_0)}] J_m(s_n \rho); \quad z' \leq z \leq c \quad (5)$$

$$\tilde{W}_{a_{mn}}^{II-} = L_{mn} e^{v_n(z-z_0)} J_m(\kappa_n \rho); \quad 0 \leq z < z' \quad (6)$$

$$\tilde{W}_{b_{mn}}^{II-} = M_{mn} e^{r_n(z-z_0)} J_m(s_n \rho); \quad 0 \leq z < z', \quad (7)$$

where $v^2 = \kappa^2 + k^2$ and $r^2 = s^2 + k^2$.

A truncation at $\rho = \rho_L$ is imposed and the truncation interface is chosen to behave as a perfect magnetic conductor (PMC). The eigenvalues κ_n and s_n are calculated by applying the PMC condition at the truncation $\rho = \rho_L$, which leads to the relations $J_m(\kappa_n \rho_L) = 0$ and $J'_m(s_n \rho_L) = 0$. The expansion coefficients $A_{mn}, B_{mn}, \dots, M_{mn}$ are determined by applying the continuity of the field at the interfaces $z = c$ and $z = z'$.

The second step of the analysis comprises the introduction of the inner and outer tube interfaces in the geometry. The perturbation due to these interfaces is expressed by the potentials $\Delta\tilde{\phi}_{mn}$ and $\Delta\tilde{W}_{a,bmn}$, the expressions of which in the regions *I* – *III* of Fig. 2 are given below:

$$\Delta\tilde{\phi}_{mn}^I = A'_{mn} \sin(w_n z) I_m(w_n \rho) \quad (8)$$

$$\Delta\tilde{\phi}_{mn}^{II} = \cos(p_n(h-z)) [B'_{mn} K_m(p_n \rho) + C'_{mn} I_m(p_n \rho)]; \quad z > c \quad (9)$$

$$\Delta\tilde{W}_{a_{mn}}^{II} = \sin(q_n z) [D'_{mn} K_m(p_n \rho) + E'_{mn} I_m(p_n \rho)]; \quad 0 \leq z < c \quad (10)$$

$$\Delta\tilde{W}_{b_{mn}}^{II} = \cos(v_n z) [L'_{mn} K_m(\xi_n \rho) + M'_{mn} I_m(\xi_n \rho)]; \quad 0 \leq z < c \quad (11)$$

$$\Delta\tilde{\phi}_{mn}^{III} = N'_{mn} \sin(w_n z) K_m(w_n \rho), \quad (12)$$

where $p^2 = q^2 + k^2$ and $v^2 = \xi^2 + k^2$. The domain is truncated at $z = h$ and $z = 0$. The PMC and PEC conditions imposed at these boundaries lead to the elimination of either the cosine or the sine term of the potentials in the air regions as well as to the determination of the eigenvalues w_n , yielding $\cos(w_n h) = 0$. Furthermore, imposing a

zero normal component of the eddy-current flow at the interface $z = c$, $J_z|_{z=c} = 0$, yields $\cos(v_n c) = 0$ from which the eigenvalues v_n are determined.

The continuity of the tangential magnetic field H_ρ and the normal magnetic flux density B_z across the conductor interface $z = c$ yields the relation between the expansion coefficients $B'_{mn} = a_n D'_{mn}$ and $C'_{mn} = a_n E'_{mn}$, where

$$a_n = \frac{q_n \cos(q_n c)}{\sin(p_n (h - c))} \quad (13)$$

as well as the transcendental equation

$$q_n \cot(q_n c) = p_n \tan(p_n (h - c)), \quad (14)$$

the numerical solution of which determines the eigenvalues p_n and q_n .

The application of the continuity of B_ρ , H_ϕ and H_z along the $\rho = b_1$ interface gives the following relations

$$\begin{aligned} \frac{h}{2} w_l I'_m(w_l b_1) A'_{ml} &= \sum_{n=1}^{\infty} S_\rho(z) \\ &+ \sum_{n=1}^{\infty} [-M_s(l, n) p_n K'_m(p_n b_1) D'_{mn} + \frac{k^2 j m}{b_1} M_r(l, n) K_m(\xi_n b_1) L'_{mn}] \\ &+ \sum_{n=1}^{\infty} [-M_s(l, n) p_n I'_m(p_n b_1) E'_{mn} + \frac{k^2 j m}{b_1} M_r(l, n) I_m(\xi_n b_1) M'_{mn}] \end{aligned} \quad (15)$$

$$\begin{aligned} \frac{h}{2} \frac{j m}{b_1} I_m(w_l b_1) A'_{ml} &= \sum_{n=1}^{\infty} S_\phi(z) \\ &+ \sum_{n=1}^{\infty} [-\frac{j m}{b_1} M_s(l, n) K_m(p_n b_1) D'_{mn} + k^2 M_r(l, n) \xi K'_m(\xi_n b_1) L'_{mn}] \\ &+ \sum_{n=1}^{\infty} [-\frac{j m}{b_1} M_s(l, n) I_m(p_n b_1) E'_{mn} + k^2 M_r(l, n) \xi I'_m(\xi_n b_1) M'_{mn}] \end{aligned} \quad (16)$$

$$\frac{h}{2} w_l I_m(w_l b_1) A'_{ml} = \sum_{n=1}^{\infty} [-M_c(l, n) p_n ((K'_m(p_n b_1) D'_{mn} + I'_m(p_n b_1) E'_{mn}) + S_z(z)), \quad (17)$$

with the mode-coupling matrices

$$M_c(l, n) = \frac{2}{h} [q_n \int_0^c \cos(q_n z) \cos(w_l z) dz + \alpha_n \int_c^h \sin(p_n (h - z)) \cos(w_l z) dz] \quad (18)$$

$$M_s(l, n) = \frac{2}{h} [p_n \int_0^c \sin(q_n z) \sin(w_l z) dz - \alpha_n \int_c^h \cos(p_n (h - z)) \sin(w_l z) dz] \quad (19)$$

$$M_r(l, n) = \frac{2}{h} \int_0^c \cos(v_n z) \cos(w_l z) dz. \quad (20)$$

and the source terms derived by the already known solution for the plate in the absence of the borehole

$$\begin{aligned}
S_\rho(z) &= [R_s^{(iii)}(-\kappa_i, w_l)A_i \\
&- R_s^{(ii)}(-v_i, w_l)v_i B_i + R_s^{(ii)}(v_i, w_l)v_i C_i + R_s^{(i)}(v_i, w_l)v_i L_i] \kappa_i J'_m(\kappa_i b_1) \\
&+ \frac{k^2 jm}{b} [R_s^{(ii)}(-r_i, w_l)D_i + R_s^{(ii)}(r_i, w_l)E_i + R_s^{(i)}(r_i, w_l)M_i] J_m(s_i b_1)
\end{aligned} \tag{21}$$

$$\begin{aligned}
S_\varphi(z) &= \frac{jm}{b_1} [R_s^{(iii)}(-\kappa_i, w_l)A_i \\
&- R_s^{(ii)}(-v_i, w_l)v_i B_i + R_s^{(ii)}(v_i, w_l)v_i C_i + R_s^{(i)}(v_i, w_l)v_i L_i] J_m(\kappa_i b_1) \\
&- k^2 [R_s^{(ii)}(-r_i, w_l)D_i + R_s^{(ii)}(r_i, w_l)E_i - R_s^{(i)}(r_i, w_l)M_i] s_i J'_m(s_i b_1)
\end{aligned} \tag{22}$$

$$\begin{aligned}
S_z(z) &= [-R_c^{(iii)}(-\kappa_i, w_l)A_i \\
&+ R_c^{(ii)}(-v_i, w_l)\kappa_i B_i + R_c^{(ii)}(v_i, w_l)\kappa_i C_i + R_c^{(i)}(v_i, w_l)\kappa_i L_i] \kappa_i J_m(\kappa_i b_1)
\end{aligned} \tag{23}$$

and

$$R_s^{(i,ii,iii)}(\mu, \nu) = \int_{0, z_0, c}^{z_0, c, h} e^{\mu(z-z_0)} \sin(\nu z) dz \tag{24}$$

$$R_c^{(i,ii,iii)}(\mu, \nu) = \int_{0, z_0, c}^{z_0, c, h} e^{\mu(z-z_0)} \cos(\nu z) dz. \tag{25}$$

The equations (15)-(17) and the three relations that yield from the continuity of B_ρ , H_φ and H_z along the $\rho = b_2$ interface and occur by replacing A'_{ml} with N'_{ml} and b_1 with b_2 in (15)-(17) form a system of equations, the solution of which defines the development coefficients $A'_{mn}, B'_{mn}, \dots, N'_{mn}$.

Having defined the expression of the potentials (3)-(7) the Green's function can be now derived according to the relation $\mathbf{E} = j\omega\mu [\nabla \times (\mathbf{e}_z W_a) + \nabla \times \nabla \times (\mathbf{e}_z W_b)]$ [4].

1.2.2. Primary field calculation

This problem differs from the one solved in 1.2.1 only in the considered field source. The coil located in region *I* of Fig. 2 is the field source, and the electric dipole in region *II* is ignored. Thus, the expression of the source potential in this case reads as

$$\tilde{\phi}_{mn}^I = A_{mn}^{(0)} \sin(w_n z) K_m(w_n \rho), \tag{26}$$

The analysis follows the same procedure as in 1.2.1 and leads to the same system of equations, where the source terms are now considered zero when matching at $\rho = b_2$, since the source is located in region *I*, and when matching the field at $\rho = b_1$ are expressed as

$$S_\rho(z) = -w_n K'_m(w_n b_1) A_{mn}^{(0)} \tag{27}$$

$$S_\varphi(z) = -\frac{jm}{b_1} K_m(w_n b_1) A_{mn}^{(0)} \tag{28}$$

$$S_z(z) = -w_n K_m(w_n b_1) A_{mn}^{(0)}, \tag{29}$$

where $A_{mn}^{(0)}$ depends only upon the coil geometry and position and it is found in [3].

1.3. Calculation of the crack response

For the calculation of the coil impedance one needs to solve an integral equation over the surface (SIM) or over the volume (VIM) of the flaw. According to the approach followed herein, the constructed Green's function is dedicated to the entire geometry of the test-piece and the only flaw considered is the crack. Thus, a surface integration (SIM) of the thin crack is applied. The crack in this analysis is discretised in a number of cells, each one including a surface dipole distribution. The integral equation that has to be solved reads as [1]

$$\mathbf{n} \cdot \mathbf{E}_0(\mathbf{r}) = -j\omega\mu_0\mathbf{n} \cdot \int_{S_{def}} G(\mathbf{r}, \mathbf{r}') \cdot \mathbf{p}(\mathbf{r}') dS_{def}, \quad (30)$$

where \mathbf{E}_0 is the electric field emitted by the probe in the absence of the crack calculated in [5], $G(\mathbf{r}, \mathbf{r}')$ is the Green's function calculated in 1.2.1 and $\mathbf{p}(\mathbf{r}')$ is the dipoles surface density representing the flaw. Finally, the impedance variation due to the crack of the probe is calculated using the reciprocity theorem [1]

$$\Delta Z_{crack} = -\frac{1}{I^2} \int_{S_{def}} \mathbf{n} \cdot \mathbf{E}_0(\mathbf{r}) \mathbf{p}(\mathbf{r}) d\mathbf{r}. \quad (31)$$

In the absence of the flaw the coil impedance variation due to the tube is determined by the expression

$$\Delta Z_{flawless} = -\frac{j\omega}{\mu_0 I^2} \pi h \sum_{m=-\infty}^{\infty} \sum_{n=1}^{\infty} A_{mn}^{(0)} A'_{mn} \quad (32)$$

2. Validation

In order to validate the presented model we compared with the results obtained using the FEM implementation of the COMSOL software. We have examined a test case of conducting tube of conductivity 10 MS/m. The tube width is 5 mm and the inner diameter is 6.25 mm. A crack of length 3 mm, depth 4 mm and opening 0.1 mm is located at the edge of the tube. The coil has an internal diameter and an external diameter of 3 mm and 5 mm, respectively, its length is 4 mm and it is wound with 336 turns. Finally, the coil center coincides with the tube axis along the whole scan and the operation frequency is 1 kHz. It is to note that the computational time of the entire scan is less than 40 seconds for the SIM method compared with the FEM model that need 60 seconds per coil position running on a computer with Intel Core i7 at 2.93GHz CPU and 8GB RAM.

Fig. 3 corresponds to the total signal ($\Delta Z = \Delta Z_{flawless} + \Delta Z_{crack}$), whereas Fig. 4 illustrates the contribution of the crack to the signal.

3. Conclusion

A fast and accurate integral equation model for the eddy-current inspection of a thin crack at the edge vicinity of a conducting tube using a dedicated Green's operator has been developed. The model considers a coil scan inside the tube and the primary field

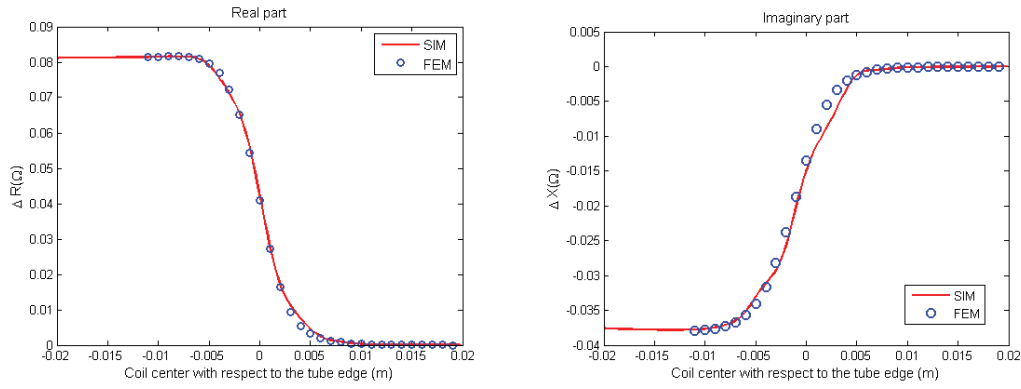


Figure 3. Comparison of the coil impedance variation of a tube with a crack at its edge as obtained from semi-analytical model following the SIM method with results obtained by COMSOL (FEM approach)

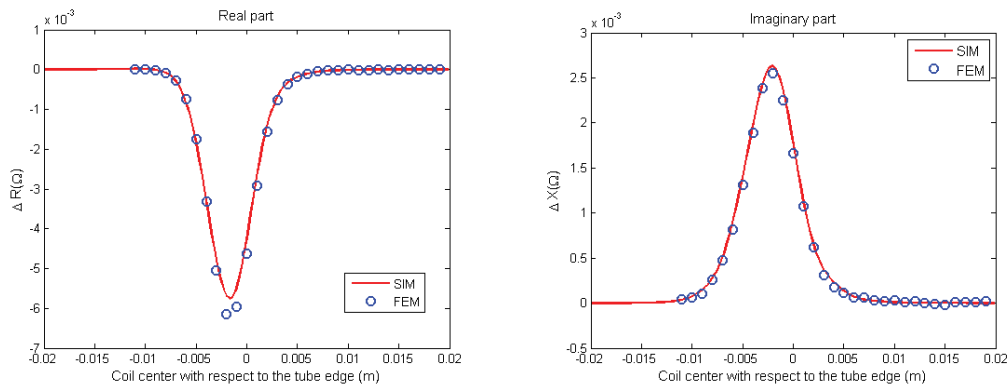


Figure 4. Contribution of the crack to the total signal as obtained from semi-analytical model following the SIM method with results obtained by COMSOL (FEM approach)

calculated with this approach can be applied in geometries of semi-infinite plates with a borehole as well [5], by considering large tube thickness compared to the penetration depth, in order to give the possibility of a scan inside the borehole (rototest). The results of this model have been compared with the results of the FEM method and a good agreement between them has been achieved.

References

- [1] R. Miorelli, C. Reboud, T. Theodoulidis, N. Poulakis and D. Lesselier, "Efficient modeling of ECT signals for realistic cracks in layered halfspace", *IEEE Trans. Magn.*, vol. 49, No. 6, pp. 2886-2892, 2013.
- [2] A. Skarlatos, G. Pichenot, D. Lesselier, M. Lambert and B. Duchêne, "Electromagnetic modeling of a damaged ferromagnetic metal tube by a volume integral equation formulation", *IEEE Trans. Magn.*, vol. 44, pp. 623-632, 2008.
- [3] T. Theodoulidis and J. Bowler, "Impedance of an induction coil at the opening of a borehole in a conductor", *J. Appl. Phys.*, vol. 103, pp. 1-9, 2008.
- [4] J. R. Bowler, T. P. Theodoulidis and N. Poulakis, "Eddy-current probe signals due to a crack at a right-angled corner", *IEEE Trans. Magn.*, vol. 48, No. 12, pp. 1-12, 2012.
- [5] A. Skarlatos and T. Theodoulidis, "Eddy-current interaction between a probe coil and a conducting plate with a cylindrical borehole", *Electromagnetic Non-Destructive Evaluation (XVI), Studies in Applied Electromagnetics and Mechanics*, vol. 38, pp. 181-188, 2014.